

ARTICLE OPEN



Source forensics of inorganic and organic nitrogen using $\delta^{15}\text{N}$ for tropospheric aerosols over Mt. Tai

Libin Wu¹, Siyao Yue², Zongbo Shi³, Wei Hu¹, Jing Chen⁴, Hong Ren¹, Junjun Deng¹, Lujie Ren¹, Yunting Fang⁵, Hong Yan⁶, Weijun Li⁷, Roy M. Harrison^{3,8} and Pingqing Fu¹✉

Nitrogen-containing species are major components in atmospheric aerosols. However, little is known about the sources of N-containing aerosols over high mountainous regions, especially for organic nitrogen (ON). This study aims to reveal the emission sources of both inorganic and organic nitrogen in tropospheric aerosols atop Mt. Tai, China, and to improve our understanding of the N cycle imbalance in the North China Plain (NCP). Total suspended particle (TSP) samples were collected on a daytime/nighttime basis in spring 2017 and were investigated for the concentrations and stable N isotopic compositions of total nitrogen, NH_4^+ , NO_3^- and ON. Our results show that the concentrations of N-containing compounds were higher in daytime than nighttime, mainly resulting from mountain–valley breezes and the changes of planetary boundary layer height. However, no significant day/nighttime changes were found for their corresponding $\delta^{15}\text{N}$ values, indicating similar contributions from different N sources between day and night. The MixSIAR Bayesian stable isotope mixing model results suggest that the most important emission source of NH_3 for aerosol NH_4^+ was agriculture, followed by fossil fuel-related sources, human waste and biomass burning. Aerosol NO_3^- was mainly formed from combustion and mobile emitted NO_x . Interestingly, the isotopes of ON suggest that ON were very likely firstly of primary origin. Our study reveals the characteristics of reactive N emission sources and helps understand the regional transport of tropospheric N-containing aerosols in the NCP.

npj Climate and Atmospheric Science (2021)4:8; <https://doi.org/10.1038/s41612-021-00163-0>

INTRODUCTION

Nitrogen (N) is a key element of life on Earth and its circulation in nature has received great attention^{1–3}. In recent years, global reactive N (N_r) emissions have increased significantly due to population growth and increased industrial and agricultural activities^{4,5}. This has caused the N cycle to become unbalanced and impact the earth's environment. In the atmosphere, excess N_r can undergo a series of chemical reactions. Surplus N_r can convert to nitrogenous substances, which are important components of atmospheric aerosols, making air pollution even more serious. In addition, N-containing aerosols can affect climate change and human health, widely participate in the N cycle and play an important role in the process of atmospheric N budget imbalance⁶. Source apportionment is a prerequisite for taking accurate measures to reduce the concentrations of N-containing aerosols in the atmosphere.

Using stable isotope techniques to identify the source and conversion process of N-containing aerosols has shown significant advantages and been a focus of recent research^{7,8}. Due to the simplicity of the test, stable N isotope analysis focused first on the measurement of total nitrogen (TN). However, the sources and components of aerosol N are very complex, with both primary emissions and secondary formation. Stable isotope analysis of TN is too broad to accurately indicate the source of N-containing aerosols. Increasing numbers of studies have focused on a single N-containing component to obtain more detailed information. In

terms of inorganic nitrogen (IN), the stable N isotope was used to analyze the source of aerosol ammonium (NH_4^+)⁷, while N and oxygen (O) isotopes were used to analyze the source and formation process of aerosol nitrate (NO_3^-)⁹. In addition to IN, organic nitrogen (ON) is also an important component of atmospheric aerosols^{10,11}, but its source apportionment has received little attention. Limited studies^{12–15} have focused on simultaneous analyses and source identification of multiple N-containing components although they are necessary for a comprehensive understanding of N-containing aerosols in the atmosphere.

Due to dense populations and severe air pollution, most research on stable isotope analyses of aerosol NH_4^+ or NO_3^- has focused on urban areas. However, the N cycle imbalance in nature affects not only urban ecosystems, but the whole earth surface and broader ecosystems^{16,17}, including rural, forest and mountain areas. The regional transport and deposition of atmospheric N-containing aerosols have a non-negligible impact on the ecological environment in these regions. For high mountain regions, air pollutants in the troposphere could be transported from the foothill area, or over a long distance at a regional scale. The mountain–valley breeze circulation would also transport air pollutants between the top and bottom of the mountain¹⁸. Stable isotopes provide useful information of the sources of multiple N-containing components in tropospheric aerosols, and a better

¹Institute of Surface-Earth System Science, School of Earth System Science, Tianjin University, Tianjin, China. ²State Key Laboratory of Atmospheric Boundary Layer Physics and Atmospheric Chemistry, Institute of Atmospheric Physics, Chinese Academy of Sciences, Beijing, China. ³Division of Environmental Health & Risk Management, School of Geography, Earth & Environmental Sciences, University of Birmingham, Birmingham, United Kingdom. ⁴School of Environmental Science and Engineering, Tianjin University, Tianjin, China. ⁵CAS Key Laboratory of Forest Ecology and Management, Institute of Applied Ecology, Chinese Academy of Sciences, Shenyang, China. ⁶State Key Laboratory of Loess and Quaternary Geology, Institute of Earth Environment, Chinese Academy of Sciences, Xi'an, China. ⁷Key Laboratory of Geoscience Big Data and Deep Resource of Zhejiang Province, Department of Atmospheric Sciences, School of Earth Sciences, Zhejiang University, Hangzhou, Zhejiang, China. ⁸Department of Environmental Sciences/Center of Excellence in Environmental Studies, King Abdulaziz University, Jeddah, Saudi Arabia. ✉email: fupingqing@tju.edu.cn

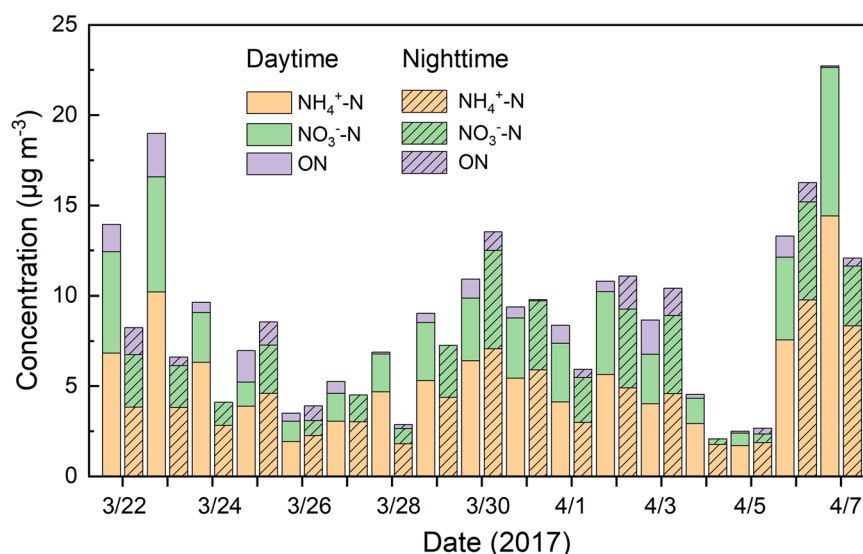


Fig. 1 The concentrations of $\text{NH}_4^+\text{-N}$, $\text{NO}_3^-\text{-N}$ and organic nitrogen (ON) in daytime and nighttime total suspended particles over Mt. Tai in spring 2017. The concentrations of ON in some samples were very low and under the detection limit, we approximate them by 0.

Table 1. Statistics (average \pm standard deviation) of the concentrations of daytime and nighttime total nitrogen (TN), inorganic nitrogen (IN: $\text{NH}_4^+\text{-N}$, $\text{NO}_3^-\text{-N}$) and organic nitrogen (ON), and corresponding isotopic compositions in total suspended particles over Mt. Tai in spring 2017.

Item	Daytime	Night time
TN ($\mu\text{g m}^{-3}$)	9.73 ± 5.27	7.14 ± 4.35
$\text{NH}_4^+\text{-N}$ ($\mu\text{g m}^{-3}$)	5.56 ± 3.13	4.09 ± 2.31
$\text{NO}_3^-\text{-N}$ ($\mu\text{g m}^{-3}$)	3.31 ± 2.04	2.62 ± 1.65
ON ($\mu\text{g m}^{-3}$)	0.86 ± 0.69	0.43 ± 1.00
$\delta^{15}\text{N-TN}$ (‰)	4.0 ± 3.1	3.4 ± 3.6
$\delta^{15}\text{N-NH}_4^+$ (‰)	6.7 ± 7.0	5.8 ± 6.7
$\delta^{15}\text{N-NO}_3^-$ (‰)	1.8 ± 2.4	1.4 ± 3.6
$\delta^{18}\text{O-NO}_3^-$ (‰)	78.5 ± 4.5	81.1 ± 4.1
$\delta^{15}\text{N-IN}$ (‰)	4.9	4.1
$\delta^{15}\text{N-ON}$ (‰)	-5.0	-7.2

understanding of the importance of N-containing aerosols in the process of atmospheric N budget imbalance.

The North China Plain (NCP) is one of three major plains in China. It has a large population, developed economy and convenient transportation links. Intensive human activities and disadvantageous natural conditions have led to the NCP being one of the severest regions with air pollution in the world in recent years^{19,20}. In addition, the NCP is a 'hot spot' for N_x emissions^{6,21}. After a large amount of N-containing substances being released into the environment, they affect the ecological environment on a larger scale through atmospheric circulation and threaten regional atmospheric N budget balance. Mt. Tai is the highest peak in the central part of the NCP (Supplementary Fig. 1)²². Since the relative height difference between the foot and top of the mountain is 1400 meters²³, it is an ideal place to study aerosols in the free troposphere and their interaction with the planetary boundary layer (PBL)²⁴. Pollutants investigated from the summit of Mt. Tai could accurately represent the characteristics of the regional pollutants in the NCP²⁵, we hypothesize that stable isotope analyses of N-containing aerosols there could indicate N_x emission sources of the whole NCP.

In this study, we collected daytime and nighttime total suspended particle (TSP) samples at the summit of Mt. Tai in spring 2017. Stable isotope analyses and a Bayesian stable isotope analysis mixing model MixSIAR were used to analyze the sources of NH_4^+ , NO_3^- and ON in TSP samples. The objectives are to quantify the main emission sources of multiple N-containing aerosols atop Mt. Tai, and reveal the characteristics of N_x emission sources of the whole NCP. Our study shows that mountain-valley breeze affects the levels but not the source attributions of N-containing aerosols over Mt. Tai, and the emission sources of tropospheric N-containing aerosols (especially NH_4^+ and ON) are somewhat different with urban aerosols in the NCP.

RESULTS

Concentrations of aerosol TN and IN

Figure 1 shows the concentrations of N-containing components in daytime and nighttime samples. The average concentrations of daytime and nighttime TN were 9.73 ± 5.27 and 7.14 ± 4.35 $\mu\text{g m}^{-3}$, respectively (Table 1). $\text{NH}_4^+\text{-N}$ was the largest distributor among the three N-containing compounds, followed by $\text{NO}_3^-\text{-N}$ and ON. Air mass backward trajectories (Supplementary Fig. 4) show that air masses were mainly from the northwest when TN was extremely low, but air masses were mainly from the east (local Shandong) when TN was extremely high. There was a significant positive correlation between the concentrations of $\text{NO}_3^-\text{-N}$ and $\text{NH}_4^+\text{-N}$ with an intercept of ~ 0 (Supplementary Fig. 5). The lowest concentrations of $\text{NO}_3^-\text{-N}$ and $\text{NH}_4^+\text{-N}$ were close to the detection limits, indicating a low level of atmospheric particulate matter pollution over Mt. Tai under favorable dispersion conditions.

The concentrations of TN, NO_3^- and NH_4^+ were higher in the daytime than the nighttime (Student's *t*-test, for TN or $\text{NH}_4^+\text{-N}$, $p < 0.05$; for $\text{NO}_3^-\text{-N}$, $p < 0.1$). This phenomenon was firstly attributed to the mountain-valley breezes. In the daytime, the valley breeze brings air masses containing particles from the foot area of Mt. Tai with intense human activities to the top, while at night, the mountain breeze reverses this transmission process. The wind rose in Supplementary Figure 3 supports this argument. Our sampling site is located at the top of the mountain, which is surrounded by terrains consisting of primarily plains with very low altitude. Therefore, the valley breeze can blow from all directions and mountain breeze can blow to all directions. Besides, the summit of Mt. Tai is within the PBL in the daytime of spring

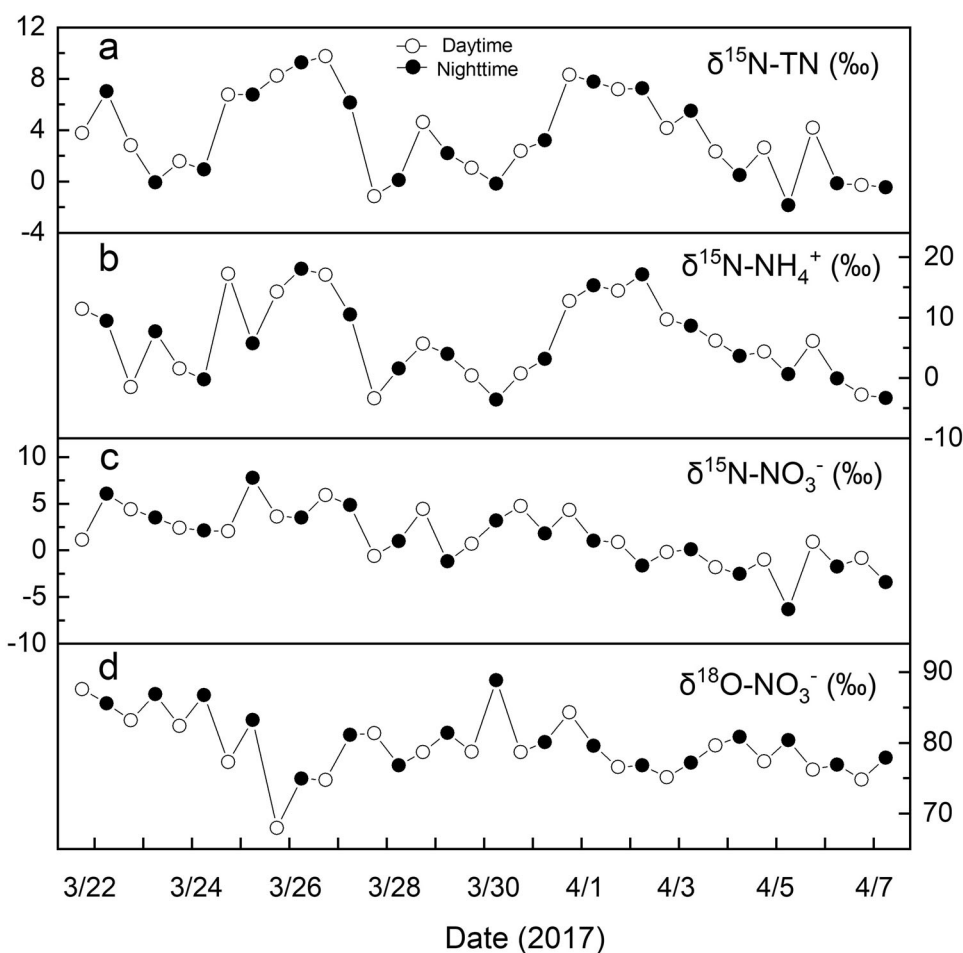


Fig. 2 Results of stable isotope analyses. Stable nitrogen isotopic compositions of **a** total nitrogen (TN) and **b** NH_4^+ , and dual isotopes (**c** $\delta^{15}\text{N}$ and **d** $\delta^{18}\text{O}$) of NO_3^- in daytime and nighttime total suspended particles over Mt. Tai in spring 2017.

season, while air mass over the summit of Mt. Tai is probably representative of the lower free troposphere at night due to the decrease of PBL height²⁶.

Stable isotopes of aerosol TN and IN

Stable N isotopic compositions of aerosol TN, NH_4^+ and NO_3^- , as well as stable O isotopic compositions of aerosol NO_3^- are presented in Fig. 2. Since NH_4^+ -N comprises the majority of TN, the trends of $\delta^{15}\text{N}$ -TN and $\delta^{15}\text{N}$ - NH_4^+ are similar to each other. On the contrary, there is an obvious difference between $\delta^{15}\text{N}$ -TN and $\delta^{15}\text{N}$ - NO_3^- . Therefore, $\delta^{15}\text{N}$ -TN is not a good indicator for the source and formation process of atmospheric N. Although the concentrations of N-containing compounds were evidently higher in daytime than nighttime, no significant diurnal change was found for their isotopic compositions (Table 1, Fig. 2. Student's *t*-test, for $\delta^{15}\text{N}$ - NH_4^+ or $\delta^{15}\text{N}$ - NO_3^- , $p > 0.1$; for $\delta^{15}\text{N}$ -TN, $p > 0.05$), suggesting little day/night difference in the source contribution of aerosol N-containing compounds.

Aerosol NH_4^+ was mainly formed from the reaction of ammonia (NH_3) and acids, and NO_3^- was mainly formed from the secondary conversion of nitrogen oxides (NO_x) in the atmosphere. There is a significant negative correlation between $\delta^{15}\text{N}$ - NH_4^+ and the concentrations of NH_4^+ -N, but no obvious correlation between $\delta^{15}\text{N}$ -TN and TN, or $\delta^{15}\text{N}$ - NO_3^- and NO_3^- -N (Supplementary Fig. 5), suggesting that the $\delta^{15}\text{N}$ value of NH_3 emissions was more variable than for NO_x . The MixSIAR source apportionment results of aerosol NH_4^+ , NO_3^- and ON are presented below.

Source apportionment of aerosol NH_4^+

There is an obvious ^{15}N fractionation factor ($\Delta^{15}\text{N} = \delta^{15}\text{N}$ - $\text{NH}_4^+ - \delta^{15}\text{N}$ - NH_3) during the gas-to-particle partitioning of NH_3 along with acids to form particulate NH_4^+ . Since the environment is an open system, a previous research studied the $\Delta\delta^{15}\text{N}$ in a dynamic chamber and found $\Delta\delta^{15}\text{N}$ was $31.6 \pm 2.0\text{‰}$ and $24.1 \pm 2.8\text{‰}$ for NH_3 turnover rate of 0.9 per day (low turnover rate) and 6.8 per day (high turnover rate), respectively²⁷. Fig. 3a, b presents the source apportionment results of aerosol NH_4^+ under two assumptions, i.e. $\Delta\delta^{15}\text{N} = 31.6 \pm 2.0\text{‰}$ and $\Delta\delta^{15}\text{N} = 24.1 \pm 2.8\text{‰}$. The contribution of livestock breeding was 42.1–48.3% and 35.8–49.0% for daytime and nighttime aerosol NH_4^+ , respectively. For N-fertilizer application, it was 11.6–13.8% and 8.1–11.0%, for daytime and nighttime respectively. Thus, the total contribution of agricultural sources was 55.9–59.9% and 43.9–60.0% for daytime and nighttime aerosol NH_4^+ , respectively. According to statistics²⁸, the output of livestock products in Shandong Province was the highest of all provinces in China and reached 8.66 million tonnes in 2017. This supports the high contribution of livestock breeding to aerosol NH_4^+ . Although the use of chemical fertilizer in Shandong Province was the second highest in China (1.39 million tonnes N fertilizer and 2.17 million tonnes compound fertilizer in Shandong in 2017)²⁸, the fertilizing amount and related NH_3 emissions were high during certain periods (e.g. summer) throughout the year. The sampling period in this study was not within the main period of fertilization in the NCP, so the contribution of N-fertilizer application in this study was not high.

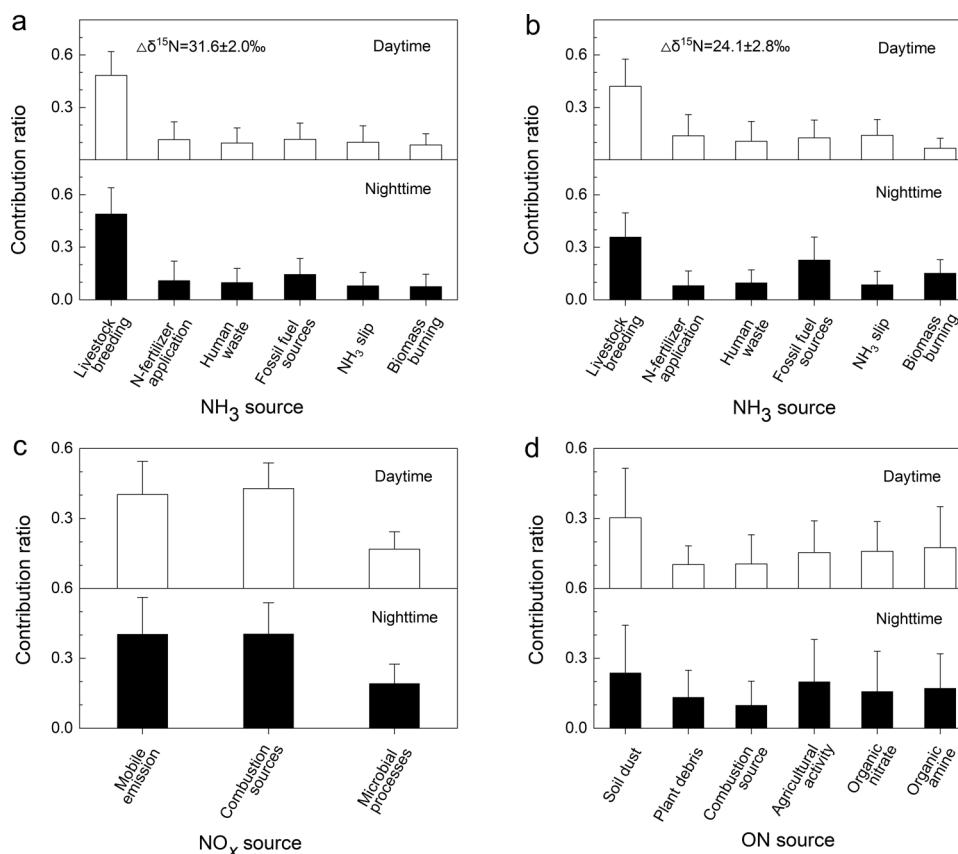


Fig. 3 Source apportionment results (average + standard deviation) of aerosol inorganic nitrogen and organic nitrogen (ON) in daytime and nighttime total suspended particles (TSP) over Mt. Tai in spring 2017, based on the MixSIAR model. Contributions of major NH₃ sources to NH₄⁺ in cases where **a** $\Delta\delta^{15}\text{N} = 31.6 \pm 2.0\text{‰}$ and **b** $\Delta\delta^{15}\text{N} = 24.1 \pm 2.8\text{‰}$, respectively; **c** contributions of major NO_x sources to NO₃⁻; **d** contributions of major sources to ON.

The contribution of fossil fuel-related sources (fossil fuel sources and NH₃ slip) was 21.9–26.7% and 22.5–31.3% for daytime and nighttime aerosol NH₄⁺, respectively, and was highly variable (Fig. 3a, b). We infer that the contribution of fossil fuel-related sources was very small compared to agricultural sources, which is consistent with a previous research²⁹. The contribution of human waste was only 9.7–10.7% and 9.7–9.9% for daytime and nighttime aerosol NH₄⁺, respectively. This source contribution atop Mt. Tai was much smaller than urban Beijing³⁰, which can be attributed to the lower population density around Mt. Tai. The contribution of biomass burning was also small, being 6.7–8.6% and 7.6–15.2% for daytime and nighttime aerosol NH₄⁺, respectively.

Source apportionment of aerosol NO₃⁻

The average aerosol $\delta^{18}\text{O}\text{-NO}_3^-$ during the entire sampling period was $78.5 \pm 4.5\text{‰}$ and $81.1 \pm 4.1\text{‰}$ for daytime and nighttime samples, respectively. Based on these values and related computational methods (Supplementary Methods)⁹, the average contributions of the two pathways NO_x + ·OH and N₂O₅ + H₂O were calculated to be 48% and 52% for daytime samples, and 43% and 57% for nighttime samples, respectively. Overall, the contributions of the two pathways were comparable. Since the production of aerosol NO₃⁻ was mainly from the NO_x + ·OH pathway in the daytime, and N₂O₅ + H₂O at night³¹, it is concluded that the aerosol NO₃⁻ in the high mountain aerosol samples was not only formed in-situ (within a few hours)³², but also transported from elsewhere. This explains why the average contribution ratio of NO_x + ·OH was comparable to N₂O₅ + H₂O for both daytime and nighttime samples.

Similar to the formation of aerosol NH₄⁺, there is also a ¹⁵N fractionation factor during the conversion of initial NO_x to aerosol NO₃⁻ (p), the average was calculated to be $5.4 \pm 8.1\text{‰}$ and $6.3 \pm 8.8\text{‰}$ for the daytime and nighttime samples, respectively, based on observed data and reported computational formulas (Supplementary Methods)⁹. Thus, the initial $\delta^{15}\text{N}\text{-NO}_x$ for daytime and nighttime aerosol NO₃⁻ was $-3.6 \pm 8.4\text{‰}$ and $-5.0 \pm 9.5\text{‰}$, respectively, there is no clear difference between these values (Student's t-test, $p > 0.1$). In the daytime, the contribution ratio of mobile emissions, combustion sources and microbial processes was $40.3 \pm 14.2\%$, $42.8 \pm 11.0\%$ and $16.9 \pm 7.4\%$, respectively. At night, the contribution of the three emission sources was $40.3 \pm 15.8\%$, $40.5 \pm 13.3\%$ and $19.2 \pm 8.3\%$, respectively (Fig. 3c). In the past decade, the NO_x emissions in Shandong Province decreased significantly³³. Previous studies pointed out that NO_x emissions from power plants and industry were the most important about 10 years before 2017³⁴. They suggested that the decrease in NO_x emissions in the NCP was mainly due to the decrease in emissions from power plants and industry, and mobile emissions have become one of the most important NO_x source. In addition, natural microbial processes might be a relatively unimportant NO_x emission source in this study, which might be due to the large population and intensive human activities in the NCP.

Stable isotopes and source apportionment of aerosol ON

As shown in Fig. 1 and Table 1, the average concentrations of ON were calculated based on the Eq. 1 to be 0.86 ± 0.69 and $0.43 \pm 1.00 \mu\text{g m}^{-3}$ for the daytime and nighttime samples, respectively. Similar to TN and IN, due to mountain–valley breezes, the concentrations of ON in the daytime was evidently higher than

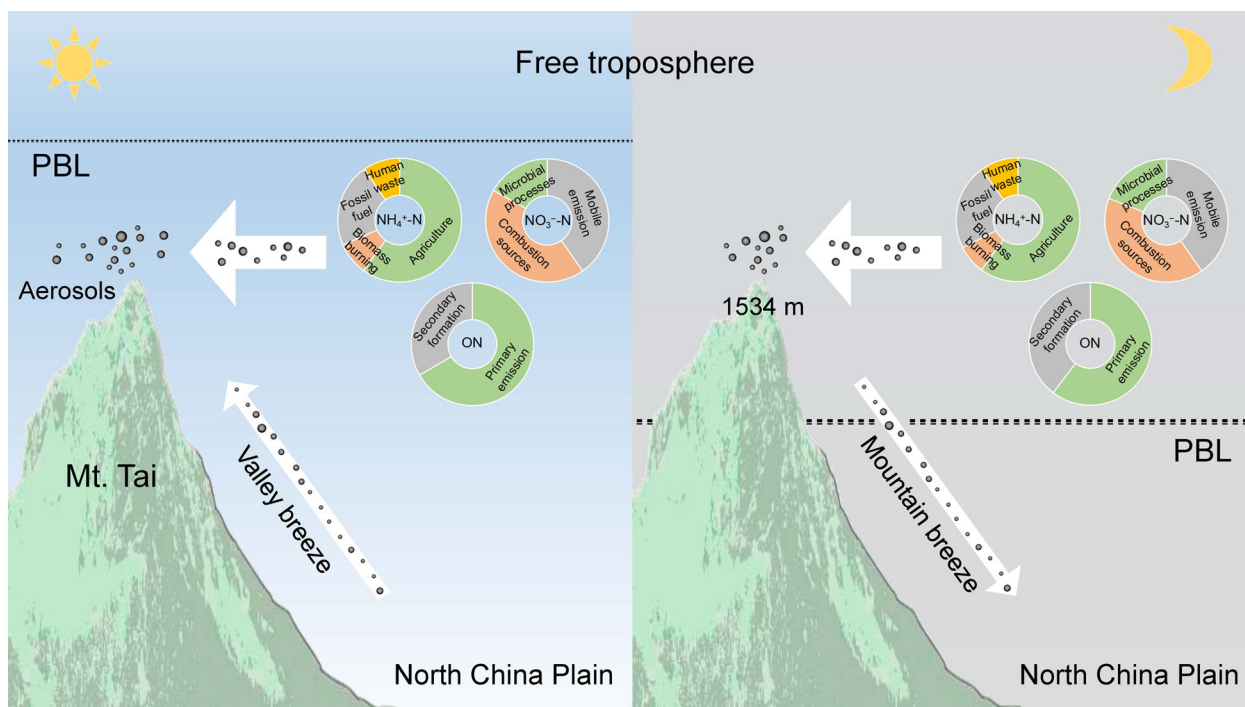


Fig. 4 A conceptual scheme of the sources and transport processes of daytime and nighttime N-containing aerosols over Mt. Tai in spring. Pie charts represent the source apportionment results of N-containing compounds in tropospheric aerosols collected atop Mt. Tai (1534 m a.s.l.). PBL planetary boundary layer; ON organic nitrogen.

those at night. It is worth pointing out that the ON content for some samples was too low to be calculated as a result of uncertainties during the calculation process, and the detection of ON using other advanced methods such as mass spectrometry is necessary. The average $\delta^{15}\text{N}$ -ON in daytime and nighttime TSP samples was calculated to be -5‰ and -7.2‰ , respectively (Table 1), based on the Eq. 2. Correspondingly, the average $\delta^{15}\text{N}$ -IN was 4.9‰ and 4.1‰ for the daytime and nighttime samples, respectively. Assuming there was no significant difference between $\delta^{15}\text{N}$ in ON and corresponding IN from secondary formation, we suggest that secondary formation was not likely the dominant source of aerosol ON.

Based on MixSIAR model, the contribution ratios of plant debris, soil dust, combustion source, agricultural activity, organic nitrate and organic amine to aerosol ON were $30.3 \pm 21.2\%$, $10.3 \pm 8.0\%$, $10.6 \pm 12.4\%$, $15.4 \pm 13.6\%$, $15.9 \pm 12.8\%$ and $17.5 \pm 17.6\%$, respectively, in the daytime; and they were $23.8 \pm 20.4\%$, $13.3 \pm 11.6\%$, $9.9 \pm 10.3\%$, $20.0 \pm 18.1\%$, $15.8 \pm 17.2\%$ and $17.2 \pm 14.7\%$ at night (Fig. 3d).

DISCUSSION

We believe the significant difference of the prevailing wind directions between day and night (Supplementary Fig. 3) was a result of mountain-valley breeze²⁶. Due to mountain breeze and the decrease of PBL height, the levels of N-containing compounds in nighttime aerosols atop Mt. Tai were lower than those in daytime. Air pollutants over spring Mt. Tai possibly come from regional transport, especially at night. Air mass backward trajectories (Supplementary Fig. 4) show that air pollutants over spring Mt. Tai possibly come from the whole NCP. Since Mt. Tai is a relatively clean area with less local pollutant emissions, the concentration of N-containing aerosols over Mt. Tai was significantly lower than that in urban areas, such as Beijing, a megacity located in the north of NCP^{35,36}. Stable isotope analyses suggested there was very small difference between the sources of daytime and nighttime N-containing aerosols. Atmospheric

particulates and therein N-containing compounds could be transported between the top and the foot of Mt. Tai. A conceptual scheme of the sources and transport processes of daytime and nighttime N-containing aerosols over spring Mt. Tai is presented in Fig. 4.

Usually, $\delta^{15}\text{N}$ - NH_3 values in agricultural emission sources were lower than non-agricultural (e.g. fossil fuel-related) sources⁷. In Beijing, since the contribution ratio of non-agricultural NH_3 emission increased with the increase of NH_4^+ -N concentrations, $\delta^{15}\text{N}$ - NH_4^+ values increased with increasing NH_4^+ -N concentrations^{7,30}. However, $\delta^{15}\text{N}$ - NH_4^+ values decreased with increasing NH_4^+ -N concentrations in this study. It is concluded that there is no significant variation in the contributions from non-agricultural NH_3 sources to NH_4^+ when particulate matter level is higher. This might be caused by that the contribution of non-agricultural NH_3 sources was small whether during non-haze or haze days atop Mt. Tai. The increase in the NH_4^+ -N concentration was partly due to the increased fraction of initial NH_3 converted to aerosol NH_4^+ , so $\Delta\delta^{15}\text{N}$ and $\delta^{15}\text{N}$ - NH_4^+ decreased^{30,37}.

Based on MixSIAR model, the contributions of different NH_3 emission sources to aerosol NH_4^+ , different NO_x emission sources to aerosol NO_3^- , and different sources to aerosol ON, were well calculated. For the source apportionment results of aerosol NH_4^+ or NO_3^- , there is an uncertainty (standard deviation) of about or less than 15% for each source (Fig. 3a-c)³⁰, but the uncertainty could reach up to 20% for aerosol ON (Fig. 3d); this mainly depends on the $\delta^{15}\text{N}$ difference among possible sources. However, we could still identify the major emission source(s) of each N-containing compound in aerosol samples, suggesting that the model is available in such studies, no matter assuming more emission sources (e.g., 6 sources) or less sources (e.g., 3 sources).

As for NH_3 emission sources to aerosol NH_4^+ over Mt. Tai, agricultural sources (livestock breeding and N-fertilizer application) were the dominant ones with livestock breeding as the most important source. Although the important or even dominant contribution of non-agricultural sources were reported in Beijing and other urban cities of the NCP^{7,30,38,39}, our results suggest that

agricultural sources of NH_3 emissions still play a major role in the whole NCP. Therefore, we conclude NH_3 emission inventories might be different in urban and the entire areas of NCP. Biomass burning is not an important source of NH_3 emission in the NCP, no matter in an urban area³⁰ or in a mountainous area surrounded by plains and countryside (this study). Overall, the source apportionment results under the assumption of $\Delta\delta^{15}\text{N} = 31.6 \pm 2.0\text{‰}$ were closer to the emission inventory^{29,40} than $\Delta\delta^{15}\text{N} = 24.1 \pm 2.8\text{‰}$. This indicates that $31.6 \pm 2.0\text{‰}$ is probably closer to the actual ^{15}N fractionation factor during the conversion of NH_3 to NH_4^+ for aerosols atop Mt. Tai, and the turnover rate of NH_3 in our study area is closer to 0.9 per day, which is considered as a low turnover rate. Thus, we conclude only a little fresh gaseous NH_3 might be added to the observed air masses during the transport of aerosol NH_4^+ .

Combustion sources (coal and biomass burning) and mobile emissions were the main emission sources of NO_x that formed aerosol NO_3^- atop Mt. Tai, their contribution ratios were very close. Since NO_x emissions are a major contributor to secondary inorganic aerosols over East Asia⁴¹, this needs to be considered when making NO_x reduction policies. Previous study showed that microbial processes contributed only a little to NO_x in spring Beijing⁴². Similar results between Beijing and Mt. Tai suggest that, anthropogenic activity, rather than microbial processes, was the dominant NO_x emission source in the NCP. Although aerosol NO_3^- over Mt. Tai has a lower concentration than urban regions³⁶, its source apportionment results partly reveal the main NO_x emission sources of the whole NCP.

Compared with previous reports, our results show that the concentrations of aerosol ON over Mt. Tai were lower than those in urban regions⁴³, but much higher than forest⁴⁴ or marine areas⁴⁵. ON accounted for 6–9% of the TN on average, which is consistent with the situation in Beijing⁴⁶. Since Mt. Tai is covered with thick vegetation and dust storm weather often occurs in NCP in spring with blooming flowers⁴⁷, plant debris (for example, pollen) and dust particles are important primary emission sources of ON. They accounted for more than one third of the total ON. Due to intensive human activities in the NCP, the contributions of agricultural activity and combustion sources (fossil fuel and biomass burning) to aerosol ON are also non-negligible. Primary emission was possibly the largest contribution to aerosol ON over Mt. Tai in spring. Around one third of ON originated from secondary formation, it was lower than the results obtained from high-resolution aerosol mass spectrometer combined with positive matrix factorization in urban Beijing (56–65%)⁴⁶. This was probably because of relatively less precursors of N-containing secondary organic aerosols, for example, volatile organic compounds, NO_x , NH_3 and soot⁴⁸, over Mt. Tai than in urban Beijing. It should be noted that high uncertainties exist in the source apportionment of ON, which warrants in-depth research in the future.

METHODS

Aerosol sampling

A total of 34 daytime and nighttime TSP samples were collected at the summit of Mt. Tai (36.26° N, 117.10° E, 1534 m a.s.l.), Shandong Province, China, from the 22nd of March to the 8th of April 2017 (Supplementary Methods)²⁶.

Chemical and isotopic analyses

$\delta^{15}\text{N}$ of NH_4^+ , $\delta^{15}\text{N}$ and $\delta^{18}\text{O}$ of NO_3^- in the aerosol samples were analyzed using a commercially available purge and cryogenic trap system coupled to an isotope ratio mass spectrometer (PT-IRMS, IsoPrime100, IsoPrime Ltd., UK). For $\delta^{15}\text{N}$ - NH_4^+ analyses, NH_4^+ was oxidized to NO_2^- by alkaline hypobromite, and then reduced to N_2O by hydroxylamine^{30,49}. $\delta^{15}\text{N}$ and $\delta^{18}\text{O}$ analyses of NO_3^- were conducted using the combination of denitrifying bacteria^{50,51} and thermal decomposition of N_2O methods^{50,52,53}.

The concentrations of NH_4^+ and NO_3^- were analyzed using a Smart Chem 200 Discrete Chemistry Analyzer (AMS, Italy).

The concentration of TN and $\delta^{15}\text{N}$ -TN were determined using a MAT 253 Isotope Ratio Mass Spectrometry (Thermo Fisher) coupled with a FLASH 2000 HT Elemental Analyzer (Thermo Fisher). The concentration of ON was obtained using TN minus IN, and $\delta^{15}\text{N}$ -ON was calculated from the concentrations and $\delta^{15}\text{N}$ values of TN and IN. Nitrite was overlooked because of its significant lower contribution to IN and possible conversion to NO_3^- during analyses. Thus, the formulas are as follows:

$$[\text{TN}] = [\text{ON}] + [\text{NH}_4^+ - \text{N}] + [\text{NO}_3^- - \text{N}] \quad (1)$$

$$[\text{TN}] \times \delta^{15}\text{N} - \text{TN} = [\text{ON}] \times \delta^{15}\text{N} - \text{ON} + [\text{NH}_4^+ - \text{N}] \times \delta^{15}\text{N} - \text{NH}_4^+ + [\text{NO}_3^- - \text{N}] \times \delta^{15}\text{N} - \text{NO}_3^- \quad (2)$$

Stable N and O isotope ratios were expressed in δ notation as the deviation from standards in parts per thousand (‰): $\delta = [(R_{\text{sample}}/R_{\text{standard}}) - 1] \times 1000\text{‰}$, where R represents the $^{15}\text{N}/^{14}\text{N}$ or $^{18}\text{O}/^{16}\text{O}$ values in the sample (R_{sample}) and in the standards (R_{standard} , atmospheric air nitrogen for $\delta^{15}\text{N}$; Vienna Standard Mean Ocean Water for $\delta^{18}\text{O}$).

NH_4^+ -N, NO_3^- -N and ON source forensics

The MixSIAR model, a Bayesian stable isotope analysis mixing model in R language³⁰, was used to determine the contributions of different emission sources to aerosol N-containing compounds (Supplementary Methods).

As stated above, ^{15}N fractionation factor ($\Delta\delta^{15}\text{N}$) during the gas-to-particle partitioning of NH_3 to form particulate NH_4^+ was $31.6 \pm 2.0\text{‰}$ and $24.1 \pm 2.8\text{‰}$ for NH_3 turnover rates of 0.9 per day and 6.8 per day, respectively²⁷. Both $\Delta\delta^{15}\text{N}$ values were used when carrying out source apportionment of aerosol NH_4^+ . We assumed that NH_3 was emitted from six major sources: volatilized livestock breeding, N-fertilizer application, human waste (including solid waste, waste water and human excreta), fossil fuel sources emitted from coal combustion and vehicle exhaust, NH_3 slip from industrial/power plants and diesel engines equipped with selective catalytic reduction techniques, and biomass burning, with mean $\delta^{15}\text{N}$ values of $-32.3 \pm 10.3\text{‰}$, $-44.8 \pm 7.4\text{‰}$, $-37.8 \pm 3.7\text{‰}$, $-3.0 \pm 3.3\text{‰}$, $-13.0 \pm 1.7\text{‰}$ and 12.0‰ , respectively^{7,14,54,55}.

The total ^{15}N fractionation factor ($\Delta\delta^{15}\text{N} = \delta^{15}\text{N}-\text{NO}_3^- (\text{p}) - \delta^{15}\text{N}-\text{NO}_x$) was calculated during the conversion process of initial NO_x (generally including NO and NO_2)⁵⁶ to particulate NO_3^- . It was assumed that NO_x was oxidized to HNO_3 (g) by two major pathways: $\text{NO}_x + \cdot\text{OH}$ and $\text{N}_2\text{O}_5 + \text{H}_2\text{O}$, there are different ^{15}N fractionation factors during these two conversion processes⁹. Contribution of the two pathways could be calculated and N isotope equilibrium fractionation of the oxidation process could be estimated, based on O isotopes. The oxidation of NO_x to HNO_3 (g) was shown to have a kinetic ^{15}N fractionation of about -3.0‰ ⁵⁷, and the conversion from HNO_3 (g) to NO_3^- (p) can have a ^{15}N equilibrium fractionation of about 21.0‰ ⁵⁷. We assumed that NO_x was emitted from three major sources: mobile emissions, combustion sources (coal combustion and biomass burning) and microbial processes, with mean $\delta^{15}\text{N}$ values of $-7.2 \pm 7.8\text{‰}$, $8.0 \pm 7.9\text{‰}$ and $-35.4 \pm 10.7\text{‰}$, respectively^{42,58–61}.

Aerosol ON could originate from primary emission of ON or secondary formation of IN⁴⁶. In this study, we assumed that primary ON was from four major sources: soil dust, plant debris, combustion source and agricultural activity, with average $\delta^{15}\text{N}$ -ON values of $2.0 \pm 1.5\text{‰}$, $-5.7 \pm 0.8\text{‰}$, $12.0 \pm 5.0\text{‰}$ and $-2.4 \pm 2.1\text{‰}$, respectively^{62–64}; and the ^{15}N fractionation between emission source and aerosol samples was ignored. Besides, we assumed that there were two categories of aerosol secondary ON: organic amine and organic nitrate, whose formation process is related to NH_3 , NH_4^+ or gaseous amine, and NO_x or NO_3^- , respectively. Due to the lack of related research and data, we supposed no difference between $\delta^{15}\text{N}$ values in aerosol NO_3^- and organic nitrate, or $\delta^{15}\text{N}$ in NH_4^+ and organic amine, in this study.

DATA AVAILABILITY

The data needed for the air mass backward trajectories was downloaded from the website of Air Resources Laboratory (<https://www.arl.noaa.gov/>). Other data used in this study are available from the corresponding author upon reasonable request.

Received: 5 July 2020; Accepted: 8 January 2021;

Published online: 17 February 2021

REFERENCES

- Stein, L. Y. & Klotz, M. G. The nitrogen cycle. *Curr. Biol.* **26**, R94–R98 (2016).
- Stüeken, E. E., Kipp, M. A., Koehler, M. C. & Buick, R. The evolution of Earth's biogeochemical nitrogen cycle. *Earth-Sci. Rev.* **160**, 220–239 (2016).
- Wu, L. B. et al. Nitrogen cycling in the soil–plant system along a series of coral islands affected by seabirds in the South China Sea. *Sci. Total Environ.* **627**, 166–175 (2018).
- Galloway, J. N. et al. Transformation of the nitrogen cycle: recent trends, questions, and potential solutions. *Science* **320**, 889–892 (2008).
- Stevens, C. J. Nitrogen in the environment. *Science* **363**, 578–580 (2019).
- Liu, X. J. et al. Atmospheric nitrogen emission, deposition, and air quality impacts in China: an overview. *Curr. Pollut. Rep.* **3**, 65–77 (2017).
- Pan, Y. P. et al. Fossil fuel combustion-related emissions dominate atmospheric ammonia sources during severe haze episodes: Evidence from ^{15}N -stable isotope in size-resolved aerosol ammonium. *Environ. Sci. Technol.* **50**, 8049–8056 (2016).
- Elliott, E. M., Yu, Z., Cole, A. S. & Coughlin, J. G. Isotopic advances in understanding reactive nitrogen deposition and atmospheric processing. *Sci. Total Environ.* **662**, 393–403 (2019).
- Zong, Z. et al. First assessment of NO_x sources at a regional background site in North China using isotopic analysis linked with modeling. *Environ. Sci. Technol.* **51**, 5923–5931 (2017).
- Zhang, Y. et al. Atmospheric organic nitrogen deposition in China. *Atmos. Environ.* **46**, 195–204 (2012).
- Jickells, T., Baker, A. R., Cape, J. N., Cornell, S. E. & Nemitz, E. The cycling of organic nitrogen through the atmosphere. *Philos. Trans. R. Soc. B* **368**, 20130115 (2013).
- Kundu, S., Kawamura, K. & Lee, M. Seasonal variation of the concentrations of nitrogenous species and their nitrogen isotopic ratios in aerosols at Gosan, Jeju Island: Implications for atmospheric processing and source changes of aerosols. *J. Geophys. Res. Atmos.* **115**, D20305 (2010).
- Shi, J. H. et al. Sources, compositions, and distributions of water-soluble organic nitrogen in aerosols over the China Sea. *J. Geophys. Res. Atmos.* **115**, D17303 (2010).
- Kawashima, H. & Kurahashi, T. Inorganic ion and nitrogen isotopic compositions of atmospheric aerosols at Yurihonjo, Japan: Implications for nitrogen sources. *Atmos. Environ.* **45**, 6309–6316 (2011).
- Luo, L. et al. Sources of reactive nitrogen in marine aerosol over the Northwest Pacific Ocean in spring. *Atmos. Chem. Phys.* **18**, 6207–6222 (2018).
- Gruber, N. & Galloway, J. N. An Earth-system perspective of the global nitrogen cycle. *Nature* **451**, 293–296 (2008).
- Canfield, D. E., Glazer, A. N. & Falkowski, P. G. The evolution and future of Earth's nitrogen cycle. *Science* **330**, 192–196 (2010).
- Bei, N. F. et al. Impacts of sea-land and mountain–valley circulations on the air pollution in Beijing–Tianjin–Hebei (BTH): a case study. *Environ. Pollut.* **234**, 429–438 (2018).
- Huang, R. J. et al. High secondary aerosol contribution to particulate pollution during haze events in China. *Nature* **514**, 218–222 (2014).
- An, Z. S. et al. Severe haze in northern China: a synergy of anthropogenic emissions and atmospheric processes. *Proc. Natl Acad. Sci. USA* **116**, 8657–8666 (2019).
- Xie, D. N., Zhao, B., Wang, S. X. & Duan, L. Benefit of China's reduction in nitrogen oxides emission to natural ecosystems in East Asia with respect to critical load exceedance. *Environ. Int.* **136**, 105468 (2020).
- Wang, G. H. et al. Water-soluble organic compounds in $\text{PM}_{2.5}$ and size-segregated aerosols over Mount Tai in North China Plain. *J. Geophys. Res. Atmos.* **114**, 1–10 (2009).
- Fu, P. Q., Kawamura, K., Chen, J. & Miyazaki, Y. Secondary production of organic aerosols from biogenic VOCs over Mt. Fuji, Japan. *Environ. Sci. Technol.* **48**, 8491–8497 (2014).
- Li, W. J., Zhang, D. Z., Shao, L. Y., Zhou, S. Z. & Wang, W. X. Individual particle analysis of aerosols collected under haze and non-haze conditions at a high-elevation mountain site in the North China Plain. *Atmos. Chem. Phys.* **11**, 11733–11744 (2011).
- Kanaya, Y. et al. Overview of the Mount Tai Experiment (MTX2006) in central East China in June 2006: studies of significant regional air pollution. *Atmos. Chem. Phys.* **13**, 8265–8283 (2013).
- Yue, S. Y. et al. Abundance and diurnal trends of fluorescent bioaerosols in the troposphere over Mt. Tai, China, in spring. *J. Geophys. Res. Atmos.* **124**, 4158–4173 (2019).
- Kawashima, H. & Ono, S. Nitrogen isotope fractionation from ammonia gas to ammonium in particulate ammonium chloride. *Environ. Sci. Technol.* **53**, 10629–10635 (2019).
- National Bureau of Statistics of China. *China Statistical Yearbook 2018* (in Chinese). (China Statistics Press, 2018).
- Huang, X. et al. A high-resolution ammonia emission inventory in China. *Glob. Biogeochem. Cy.* **26**, GB1030 (2012).
- Wu, L. B. et al. Aerosol ammonium in the urban boundary layer in Beijing: Insights from nitrogen isotope ratios and simulations in summer 2015. *Environ. Sci. Technol. Lett.* **6**, 389–395 (2019).
- Leighton, P. A. Sunlight and health hazards (Book reviews: Photochemistry of air pollution). *Science* **135**, 427–428 (1962).
- Lelieveld, J. & Poeschl, U. Chemists can help to solve the air-pollution health crisis. *Nature* **551**, 291–293 (2017).
- Shandong Provincial Bureau of Statistics & Survey Office of the National Bureau of Statistics in Shandong. *Shandong Statistical Yearbook 2018* (in Chinese). (China Statistics Press, 2018).
- Zhang, Q. et al. Asian emissions in 2006 for the NASA INTEX-B mission. *Atmos. Chem. Phys.* **9**, 5131–5153 (2009).
- Wei, L. F. et al. Gas-to-particle conversion of atmospheric ammonia and sampling artifacts of ammonium in spring of Beijing. *Sci. China Earth Sci.* **58**, 345–355 (2015).
- Luo, L. et al. Origins of aerosol nitrate in Beijing during late winter through spring. *Sci. Total Environ.* **653**, 776–782 (2019).
- Heaton, T. H. E., Spiro, B. & Roberston, S. M. C. Potential canopy influences on the isotopic composition of nitrogen and sulphur in atmospheric deposition. *Oecologia* **109**, 600–660 (1997).
- Zhang, Y. Y. et al. Persistent non-agricultural and periodic agricultural emissions dominate sources of ammonia in urban Beijing: Evidence from ^{15}N stable isotope in vertical profiles. *Environ. Sci. Technol.* **54**, 102–109 (2020).
- Zhang, Z. Y. et al. Fossil fuel-related emissions were the major source of NH_3 pollution in urban cities of northern China in the autumn of 2017. *Environ. Pollut.* **256**, 113428 (2020).
- Zhang, X. M. et al. Ammonia emissions may be substantially underestimated in China. *Environ. Sci. Technol.* **51**, 12089–12096 (2017).
- Kharol, S. K. et al. Persistent sensitivity of Asian aerosol to emissions of nitrogen oxides. *Geophys. Res. Lett.* **40**, 1021–1026 (2013).
- Zong, Z. et al. Dual-modelling-based source apportionment of NO_x in five Chinese megacities: Providing the isotopic footprint from 2013 to 2014. *Environ. Int.* **137**, 105592 (2020).
- Ho, S. S. H. et al. Seasonal behavior of water-soluble organic nitrogen in fine particulate matter ($\text{PM}_{2.5}$) at urban coastal environments in Hong Kong. *Air Qual. Atmos. Hlth.* **12**, 389–399 (2019).
- Miyazaki, Y., Fu, P., Ono, K., Tachibana, E. & Kawamura, K. Seasonal cycles of water-soluble organic nitrogen aerosols in a deciduous broadleaf forest in northern Japan. *J. Geophys. Res. Atmos.* **119**, 1440–1454 (2014).
- Mace, K. A., Duce, R. A. & Tindale, N. W. Organic nitrogen in rain and aerosol at Cape Grim, Tasmania, Australia. *J. Geophys. Res. Atmos.* **108**, 4338 (2003).
- Xu, W. et al. Seasonal characterization of organic nitrogen in atmospheric aerosols using high resolution aerosol mass spectrometry in Beijing, China. *ACS Earth Space Chem.* **1**, 673–682 (2017).
- Long, X. et al. Effect of ecological restoration programs on dust concentrations in the North China Plain: a case study. *Atmos. Chem. Phys.* **18**, 6353–6366 (2018).
- Cape, J. N., Cornell, S. E., Jickells, T. D. & Nemitz, E. Organic nitrogen in the atmosphere—Where does it come from? A review of sources and methods. *Atmos. Res.* **102**, 30–48 (2011).
- Liu, D. W., Fang, Y. T., Tu, Y. & Pan, Y. P. Chemical method for nitrogen isotopic analysis of ammonium at natural abundance. *Anal. Chem.* **86**, 3787–3792 (2014).
- Kaiser, J., Hastings, G. M., Houlton, Z. B., Thomas, R. & Dainel, M. S. Triple oxygen isotope analysis of nitrate using the denitrifier method and thermal decomposition of N_2O . *Anal. Chem.* **79**, 599–607 (2007).
- Sigman, D. M. et al. A bacterial method for the nitrogen isotopic analysis of nitrate in seawater and freshwater. *Anal. Chem.* **73**, 4145–4153 (2001).
- Smirnov, A., Savard, M. M., Vet, R. & Simard, M. C. Nitrogen and triple oxygen isotopes in near-road air samples using chemical conversion and thermal decomposition. *Rapid Commun. Mass Spectrom.* **26**, 2791–2804 (2012).
- Li, Z. J. et al. Nitrate isotopic composition in precipitation at a Chinese megacity: seasonal variations, atmospheric processes and implications for sources. *Earth Space Sci.* **6**, 2200–2213 (2019).
- Felix, J. D., Elliott, E. M., Gish, T. J., McConnell, L. L. & Shaw, S. L. Characterizing the isotopic composition of atmospheric ammonia emission sources using passive samplers and a combined oxidation-bacterial denitrifier approach. *Rapid Commun. Mass Spectrom.* **27**, 2239–2246 (2013).
- Chang, Y. H., Liu, X. Y., Deng, C. R., Dore, A. J. & Zhuang, G. S. Source apportionment of atmospheric ammonia before, during, and after the 2014 APEC summit in Beijing using stable nitrogen isotope signatures. *Atmos. Chem. Phys.* **16**, 11635–11647 (2016).
- van der A, R. J., de Laat, A. T. J., Ding, J. & Eskes, H. J. Connecting the dots: NO_x emissions along a West Siberian natural gas pipeline. *npj Clim. Atmos. Sci.* **3**, 16 (2020).
- Freyer, H. Seasonal variation of $^{15}\text{N}/^{14}\text{N}$ ratios in atmospheric nitrate species. *Tellus B* **43**, 30–44 (1991).

58. Felix, J. D., Elliott, E. M. & Shaw, S. L. Nitrogen isotopic composition of coal-fired power plant NO_x: Influence of emission controls and implications for global emission inventories. *Environ. Sci. Technol.* **46**, 3528–3535 (2012).
59. Felix, J. D. & Elliott, E. M. Isotopic composition of passively collected nitrogen dioxide emissions: vehicle, soil and livestock source signatures. *Atmos. Environ.* **92**, 359–366 (2014).
60. Walters, W. W., Goodwin, S. R. & Michalski, G. Nitrogen stable isotope composition ($\delta^{15}\text{N}$) of vehicle-emitted NO_x. *Environ. Sci. Technol.* **49**, 2278–2285 (2015).
61. Fibiger, D. L. & Hastings, M. G. First measurements of the nitrogen isotopic composition of NO_x from biomass burning. *Environ. Sci. Technol.* **50**, 11569–11574 (2016).
62. Bateman, A. S. & Kelly, S. D. Fertilizer nitrogen isotope signatures. *Isot. Environ. Health Stud.* **43**, 237–247 (2007).
63. Kang, H. et al. Variation in foliar $\delta^{15}\text{N}$ among oriental oak (*Quercus variabilis*) stands over eastern China: Patterns and interactions. *J. Geochem. Explor.* **110**, 8–14 (2011).
64. Liu, X. Y. et al. Stable isotope analyses of precipitation nitrogen sources in Guiyang, southwestern China. *Environ. Pollut.* **230**, 486–494 (2017).

ACKNOWLEDGEMENTS

This work was supported by the National Key R&D Program of China (Grant No. 2017YFC0212700), the National Natural Science Foundation of China (Grant Nos. 41905110, 41625014, and 41961130384), the Royal Society Newton Advanced Fellowship (Grant No. NAFR1\191220) and State Key Laboratory of Loess and Quaternary Geology, Institute of Earth Environment, Chinese Academy of Sciences (Grant No. SKLLQG1837). The authors received support from Shanfeng Yuan of Institute of Atmospheric Physics, Chinese Academy of Sciences for meteorological data.

AUTHOR CONTRIBUTIONS

P.F. and L.W. conceived the study. P.F., R.M.H. and Y.F. supported the study. S.Y., H.R., J.C., L.R. and W.L. conducted the field work. L.W. and S.Y. conducted experiments and analyses. L.W. wrote the paper with contribution and review from all coauthors.

COMPETING INTERESTS

The authors declare no competing interest.

ADDITIONAL INFORMATION

Supplementary information The online version contains supplementary material available at <https://doi.org/10.1038/s41612-021-00163-0>.

Correspondence and requests for materials should be addressed to P.F.

Reprints and permission information is available at <http://www.nature.com/reprints>

Publisher's note Springer Nature remains neutral with regard to jurisdictional claims in published maps and institutional affiliations.



Open Access This article is licensed under a Creative Commons Attribution 4.0 International License, which permits use, sharing, adaptation, distribution and reproduction in any medium or format, as long as you give appropriate credit to the original author(s) and the source, provide a link to the Creative Commons license, and indicate if changes were made. The images or other third party material in this article are included in the article's Creative Commons license, unless indicated otherwise in a credit line to the material. If material is not included in the article's Creative Commons license and your intended use is not permitted by statutory regulation or exceeds the permitted use, you will need to obtain permission directly from the copyright holder. To view a copy of this license, visit <http://creativecommons.org/licenses/by/4.0/>.

© The Author(s) 2021